Analysis of Flexible-Membrane and Jet-Flapped Airfoils Using Velocity Singularities

D. Mateescu* and B. G. Newman†
McGill University, Montreal, Quebec H3A 2K6, Canada

A method for predicting the flow past thin airfoils in incompressible potential flow is presented. This method makes use of special singularities that directly represent the complex conjugate perturbation velocity in the plane of the airfoil. The method is developed first for rigid cambered airfoils and is then extended to problems for which it is particularly suitable, namely, the flow past flexible impervious membranes and past airfoils with jet flaps.

Nomenclature

a = coefficient of the trailing-edge singularity in Eq. (47); inversely proportional to C_J from Eq. (57)
C_J = nondimensional jet momentum coefficient, $2J/(\rho U^2 c)$
C_L = nondimensional lift coefficient, $2L/(\rho U^2 c)$
C_m = nondimensional moment coefficient, $2M/(\rho U^2 c^2)$
C_p = nondimensional pressure coefficient, $2(p-p_\infty)/(\rho U^2)$
C_T = nondimensional tension coefficient for a membrane airfoil, $2T/(\rho U^2 c)$
c = airfoil chord
$e(X)$ = shape of the jet sheet, $y=e(X)$
$h(X)$ = shape of the camberline, $y=h(X)$
I_k = is defined by Eq. (55)
J_k = is defined by Eqs. (35) and (56)
L = downstream end of the jet sheet (with respect to the leading edge), where the jet curvature has become effectively zero and the slope is parallel to the freestream velocity; ℓ/c
R = local radius of curvature of a membrane or a jet sheet
S = nondimensional coordinate indicating the position of the ridge, s/c
s = position of a ridge ($x=s$); also, position of elementary ridges representing a continuously cambered airfoil (rigid or otherwise)
U = freestream velocity
u = perturbation velocity in the chordwise direction
v = perturbation velocity in the y direction
v_b = value of v at a solid boundary
v_0 = value of v at the leading edge
w = complex conjugate perturbation velocity, $u-i(v-v_0)$
X = nondimensional coordinate, x/c
x = chordwise coordinate from leading edge (Figs. 1 and 3)
y = coordinate perpendicular to x axis (Figs. 1 and 3)
z = complex variable with origin at the leading edge, $x+iy$
α = incidence with respect to the upstream flow velocity U
β = change of slope at a ridge ($x=s$); also, the slope of the jet flap at the trailing edge relative to the chord (Fig. 3)
ΔC_p = nondimensional pressure difference across the airfoil, $C_{p_{\text{lower}}}-C_{p_{\text{upper}}}=2\Delta p/(\rho U^2)$
Δv = change of v at the ridge, $-\beta U$
ζ = auxiliary transformed plane defined by Eq. (7), $\xi+i\eta$
σ = ridge position in the auxiliary plane ζ, $\sqrt{s/(c-s)}$
τ = leading-edge slope relative to the chord

Received Aug. 21, 1990; revision received Nov. 26, 1990; accepted for publication Nov. 26, 1990.

*Associate Professor, Department of Mechanical Engineering, 817 Sherbrooke Street West. Member AIAA.
†Professor, Department of Mechanical Engineering, 817 Sherbrooke Street West.

Introduction

A THIN airfoil theory is presented in this paper that is particularly suitable for problems in which the boundary conditions can be stated in terms of either the slope or the change of slope of the surface. Special singularities directly represent the complex conjugate velocity perturbations due to the airfoil.

Classical thin airfoil theory for a rigid airfoil was given by Birnbaum and Glauert[1] using a modified Fourier expansion for the distribution of circulation. Stewart[2] has modified the method by transforming the airfoil to the circle plane, and stating the complex velocity perturbation as a series of singularities in this plane. The final results are expressed as a modified Fourier series for the pressure difference, which is identical to Glauert's expression for the distribution of circulation. Other efficient methods using numerical techniques have been developed more recently for airfoils of any thickness and camber; for example, Halsey[3] uses a numerically computed conformal transformation for the conventional complex potential. Boundary element methods developed in the form of panel methods based on source and doublet, or vortex, distributions have also been used for various aeronautical applications.[4,5]

In the present method, special singularities are used to determine the complex conjugate perturbation velocity $u-iv$ (rather than the complex potential) in the airfoil plane. This approach has two advantages: solutions are obtained in terms of polynomial expansions rather than Fourier series, and it is easier to satisfy the boundary conditions, particularly when their position is not known a priori (e.g., jet flap or flexible-membrane airfoils).

The simplest prototype problem is that of a very thin airfoil extending on the real axis in the complex plane $z=x+iy$ from $z=0$ to $z=c$ with a sudden change of slope, due to a single ridge, at $z=s$ (Fig. 1). As shown in the next section, two velocity singularities are required that are proportional to the following:

At the leading edge, $z=0$

$$\sqrt{\frac{(c-z)}{z}}$$

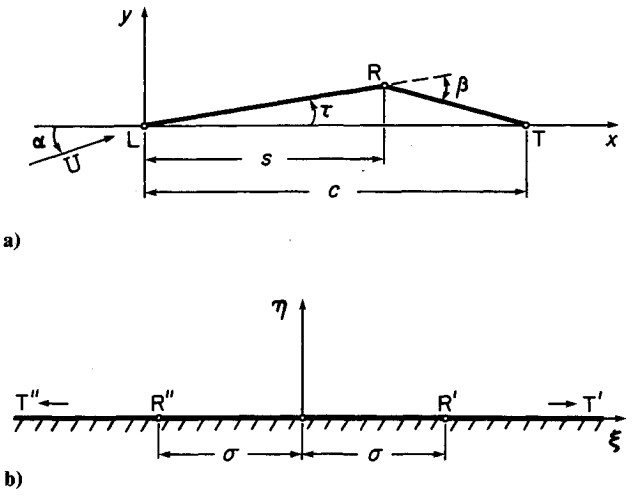

Fig. 1 Geometry of a thin flapped airfoil: a) in the physical complex plane $z=x+iy$; b) in the complex plane $\zeta=\xi+i\eta$ defined by the conformal transformation (7).

At the ridge, $z=s$ $(0<s<c)$

$$\cosh^{-1}\sqrt{\frac{(c-z)s}{c(s-z)}}$$

Note that both of these singularities also automatically satisfy the Kutta condition at $z=c$. This type of approach is similar to that developed by Carafoli and Mateescu[6,7] for supersonic conical flows, although for those cases the singular contributions were derived in a crossflow plane and from different initial equations.

The prototype solution is readily generalized to a continuously cambered rigid airfoil, since the v component of velocity (normal to the chord) is directly proportional to the local slope. Solutions for circular arcs are compared with the classical results.

Problems involving either two-dimensional flexible membranes[8] or airfoils with jet flaps have a boundary condition in which the pressure difference across the membrane or the jet (proportional to the chordwise perturbation velocity u) is proportional to the local curvature (or the rate of change of the airfoil slope). Solutions are obtained for both of these problems for which the airfoil shape is initially unknown. These predictions are then compared with previous results obtained by Nielsen[9] and Thwaites[10] for membrane airfoils and by Spence[11-14] for jet-flapped airfoils.

Method of Solution Using Velocity Singularities

Prototype Problem

A typical configuration of a flapped, otherwise uncambered, airfoil (Fig. 1a) is first considered. This gives the basic singularities at the leading edge $L(x=0)$ and at the ridge $R(x=s)$, where the airfoil slope suddenly changes by an angle β. The boundary conditions are

$$v=\begin{cases}U(\tau-\alpha)=v_0 & \text{for } 0<x<s\\ U(\tau-\alpha-\beta)=v_0+\Delta v & \text{for } s<x<c\end{cases} \tag{1}$$

where α is the angle of attack, τ is the leading-edge slope with respect to the chord, $v_0=U(\tau-\alpha)$ represents the normal-to-chord perturbation velocity v at the leading edge and $\Delta v=-\beta U$ denotes the change in v at the ridge. In the complex plane $z=x+iy$, the conjugate complex perturbation velocity is defined as

$$w(z)=u-i(v-v_0) \tag{2}$$

The boundary conditions (1) applied on the airfoil chord are, thereby, simplified to

$$\text{IMAG}\left[w(z)\right]_{z=x}=\begin{cases}0 & \text{for } 0<x<s\\ -\Delta v & \text{for } s<x<c\end{cases} \tag{3}$$

and, due to the antisymmetric nature of the perturbation flow past the airfoil in the complex plane,

$$\text{REAL}\left[w(z)\right]_{z=x}=0 \qquad \text{for } x<0,\quad x>c \tag{4}$$

The local behavior of the perturbation velocities at the leading and trailing edges are, respectively

$$w(z)|_{z\to 0}\to\frac{A_0}{\sqrt{z}} \qquad \begin{matrix}(\text{where } A_0 \text{ is independent of } z)\\ \text{REAL}\left[w(z)\right]_{z\to c}=0\end{matrix} \tag{5}$$

where the first condition represents the leading-edge singularity for a flat plate at $z=0$ (Ref. 1), and the second is the Kutta condition at the trailing edge $(z=c)$. The complex velocity $w(z)$ should also contain a logarithmic singularity in order to provide the jump Δv at the ridge $(z=s)$:

$$w(z)|_{z\to s}=\frac{\Delta v}{\pi}\ell n(z-s) \tag{6}$$

The expression of $w(z)$ is determined in an auxiliary plane $\zeta=\xi+i\eta$ (Fig. 1b), defined by the conformal transformation of the Schwarz-Christoffel type[1]

$$\zeta^2=z/(c-z) \tag{7}$$

which transforms the airfoil (the x axis between 0 and c) into the whole of the real axis in the ζ plane, and the rest of the x axis into the imaginary axis. Noting that, in this theory, the velocity components do not change under conformal transformation in contrast to the usual complex potential theory, the boundary conditions become

$$\text{IMAG}[w]_{\eta=0}=\begin{cases}0 & \text{for } -\sigma<\xi<\sigma\\ -\Delta v & \text{for } \xi<-\sigma,\ \zeta>\sigma\end{cases} \tag{8}$$

$$\left[\text{where } \sigma=\sqrt{s/(c-s)}\right]$$

$$\text{REAL}[w]_{\xi=0}=0 \tag{9}$$

The leading-edge singularity becomes a doublet singularity $1/\zeta$ at the origin, and the ridge singularity becomes in this plane $\pm(\Delta v/\pi)\ell n(\zeta\mp\sigma)$, and, thus,

$$w=A\frac{1}{\zeta}+\frac{\Delta v}{\pi}\left[\ell n\frac{\zeta-\sigma}{\zeta+\sigma}-i\pi\right] \tag{10}$$

where the constant A has to be determined.

In the physical complex plane z, the solution becomes

$$w(z)=A\sqrt{\frac{c-z}{z}}-\frac{2}{\pi}\Delta v\cosh^{-1}\sqrt{\frac{(c-z)s}{c(s-z)}} \tag{11}$$

and the constant A comes from the requirement that $u=v=0$ at $z\to-\infty$, resulting in

$$A=-v_0-\frac{2}{\pi}\Delta v\cos^{-1}\sqrt{\frac{s}{c}}=U\left[\alpha-\tau+\frac{2}{\pi}\beta\cos^{-1}\sqrt{\frac{s}{c}}\right] \tag{12}$$

On the upper surface of the airfoil $(y=0,\ z=x)$, the chordwise perturbation velocity $u=\text{REAL}\ w(z)$ may, therefore, be expressed as

$$u(x)=A\sqrt{\frac{c-x}{x}}-\frac{2}{\pi}\Delta v G(c,s,x) \tag{13}$$

where the singular ridge contribution $G(c,s,x)$ is defined as

$$G(c,s,x)=\begin{cases}\cosh^{-1}\sqrt{\dfrac{(c-x)s}{c(s-x)}} & \text{for } 0<x<s\\ \sinh^{-1}\sqrt{\dfrac{(c-x)s}{c(x-s)}} & \text{for } s<x<c\\ 0 & \text{for } x<0 \text{ and } x>c\end{cases} \tag{14}$$

The pressure difference across the airfoil in dimensionless form $\Delta C_p=4u/U$, where $\pm u$ are the chordwise perturbation velocity components on the upper and lower surfaces of the airfoil, can now be expressed as

$$\Delta C_p(x)=-\frac{4}{U}\left[\left(v_0+\frac{2}{\pi}\Delta v\cos^{-1}\sqrt{\frac{s}{c}}\right)\sqrt{\frac{c-x}{x}}+\frac{2}{\pi}\Delta v G(c,s,x)\right] \tag{15}$$

where $v_0=(\tau-\alpha)U$ and $\Delta v=-\beta U$.

The lift coefficient and the pitching moment coefficient about the leading edge are obtained by integration of the pressure coefficient over the airfoil:

$$C_L=2\pi(\alpha-\tau)+4\beta\left[\cos^{-1}\sqrt{\frac{s}{c}}+\sqrt{\frac{s}{c}\left(1-\frac{s}{c}\right)}\right]$$

$$C_m=\frac{1}{4}C_L+2\beta\left(\frac{s}{c}\right)^{3/2}\left(1-\frac{s}{c}\right)^{1/2} \tag{16}$$

These expressions are essentially the same as those derived from Glauert's thin airfoil theory[15] using a modified Fourier expansion with N terms [see Eq. (26)]. However, there are significant differences between the local pressure differences $\Delta C_p(x)$ provided by the present closed-form solution (15) and Glauert's method [which cannot represent accurately the jump in the boundary conditions (1) at $x=s$]. This is shown in Fig. 2 for a flapped airfoil with $\alpha=0$, $\beta=0.1$ rad, and $s/c=0.6$. One can notice that the results obtained with Glauert's theory using an increasing number of terms, $(N+1)$, in the Fourier expansion oscillate about the present closed-form solution (for the chordwise locations $x/c=0.55$ and 0.65), or tend asymptotically, but very slowly, toward the present solution ($x/c=0.601$).

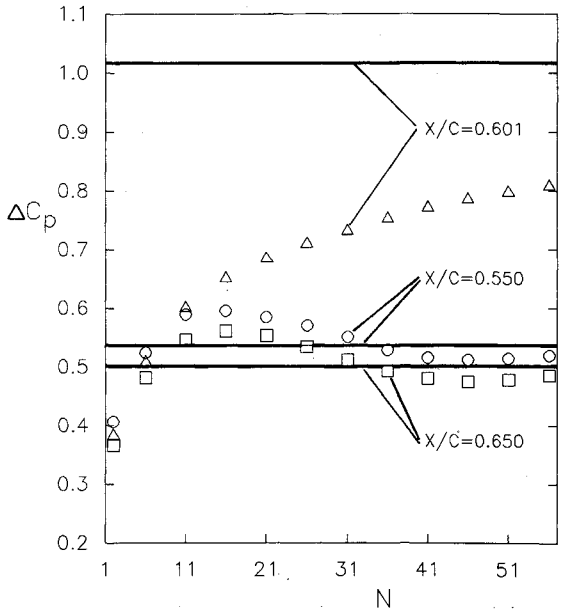

Fig. 2 Comparison between the present solution in closed form (—) and Glauert's solution (○, □, and Δ) based on a modified Fourier expansion with various numbers of terms N for the nondimensional pressure difference ΔC_p across a flapped airfoil ($\alpha=0$, $\beta=0.1$ rad, $s/c=0.6$) at three chordwise locations, $x/c=0.55$, 0.601, and 0.65.

Continuously Cambered Airfoils

The method is easily extended to thin continuously cambered airfoils, defined by the camber slope $h'(X)=\alpha+v_b(X)/U$, where v_b is the normal-to-chord perturbation velocity v at the solid boundary, and $X=x/c$ is a nondimensional coordinate. Using the two typical singular contributions for the leading edge and ridge, the solution for any camberline shape can be obtained by superimposing infinitesimally flapped airfoils [Eq. (15)] in the form

$$\Delta C_p(X)=-\frac{4}{U}\left\{\left[v_b(0)+\frac{2}{\pi}\int_0^1 v_b'(S)\cos^{-1}\sqrt{S}\,dS\right]\sqrt{\frac{1-X}{X}}+\frac{2}{\pi}\int_0^1 v_b'(S)G(1,S,X)\,dS\right\} \tag{17}$$

where $X=x/c$ and $S=s/c$.

Considering a polynomial representation for the camberline slope (which was also adopted in the design of the NACA 5 digit airfoil series),

$$h'(X)=\frac{1}{U}v_b(X)+\alpha=\sum_{k=0}^{n}h_kX^k \tag{18}$$

the pressure difference across the airfoil is obtained in nondimensional form as

$$\Delta C_p(X)=4\left[\alpha-\sum_{k=0}^{n}h_k\sum_{j=0}^{k}g_{k-j}X^j\right]\sqrt{\frac{1-X}{X}} \tag{19}$$

where

$$g_q=\frac{1\cdot3\cdot5\cdots(2q-1)}{2\cdot4\cdot6\cdots(2q)}=\frac{(2q)!}{2^{2q}(q!)^2},\qquad g_0=1 \tag{20}$$

The lift and pitching moment coefficients are

$$C_L=2\pi\left[\alpha-2\sum_{k=0}^{n}h_kg_{k+1}\right] \tag{21}$$

$$C_m=\frac{\pi}{2}\left[\alpha-4\sum_{k=0}^{n}h_kg_{k+1}\frac{k+1}{k+2}\right] \tag{22}$$

A numerical comparison made for a circular arc airfoil (camber ratio $f/c=0.02$ and incidence $\alpha=0.1$ rad) indicated that the present solution was in very good agreement with the exact solution obtained by conformal transformation. The agreement in the chordwise distribution of the pressure coefficient was within ±1% (in fact, much better on most of the chord), and the difference between the calculated lift and pitching moment coefficients was smaller than 0.05%.

Membrane Airfoils

When the airfoil is a flexible, impervious, and nonstretchable membrane (or a two-dimensional sail, as shown in Fig. 3a), its shape is unknown but it has to satisfy the normal equilibrium equation between the tension and the local pressure difference across the membrane (see Refs. 9, 10, 16–18):

$$\Delta p=\frac{T}{R}\approx -Th''(x) \tag{23}$$

The latter approximation for the radius of curvature R is for small slopes. The tension T, per unit span, can be considered constant since the skin friction is zero in theory and very small in practice.

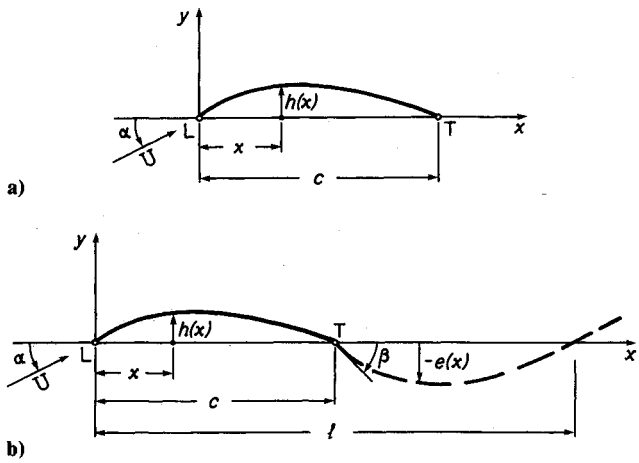

Fig. 3 Geometry of a) a flexible membrane airfoil and b) a thin jet-flapped airfoil.

Introducing the nondimensional coefficients $\Delta C_p = 2\Delta p/(\rho U^2)$ and $C_T = 2T/(\rho U^2 c)$, where c is the chord length, Eq. (23) becomes

$$\Delta C_p = -cC_T h''(x) \tag{24}$$

where the nondimensional pressure difference is $\Delta C_p = 4u/U$. The aerodynamic boundary condition on the airfoil is expressed in terms of the normal perturbation velocity component v in the form

$$v = v_b(x) \approx \left[-\alpha + h'(x)\right] U \tag{25}$$

Nielsen[9] treated this problem by using Glauert's approach based on a modified Fourier expansion for the circulation $\gamma = 2U\Delta C_p$ in the form

$$\Delta C_p = \frac{\gamma}{2U} = A_0 \tan\frac{\theta}{2} + \sum_{k=1}^{N} A_k \sin k\theta \tag{26}$$

where the coefficients A_0 and A_k are related to the cosine Fourier expansion of the airfoil slope, $h'(x)$, in terms of the variable $\theta = \cos^{-1}(2x/c - 1)$ in the form

$$\alpha - h'(x) = A_0 + \sum_{k=1}^{N} A_k \cos k\theta \tag{27}$$

On this basis, Eq. (24) was rewritten as

$$\frac{1}{2} C_T \sum_{k=1}^{N} kA_k \sin k\theta = A_0(1-\cos\theta) + \sin\theta \sum_{k=1}^{N} A_k \sin k\theta \tag{28}$$

which had to be used to determine the coefficients A_0 and A_k that define the membrane shape.

However, at the leading edge, $\theta = \pi$, Eq. (28) leads to $A_0 = 0$, which corresponds to the ideal incidence for which the Kutta condition is also satisfied at the leading edge. At any other incidence, the constant A_0 should not be zero, and then Eq. (28) is not satisfied at the leading edge. Nielsen[9] avoided this particular difficulty by expanding each term of Eq. (28), including 1 and $\cos\theta$, as sine Fourier series, and equating the coefficients of $\sin k\theta$.

The present method does not contain the above ambiguity. By differentiating Eq. (25), the membrane equilibrium equation (24) may be recast only in terms of u and v as

$$h''(x) = v_b'(x)/U = -\frac{4}{cC_T}\frac{u(x)}{U} \tag{29}$$

For any shape of the camberline, Eq. (17) shows that u contains the factor $\sqrt{(1-X)/X} = \sqrt{(c-x)/x}$, which satisfies the Kutta condition at $X = 1$ and has the $X^{-1/2} = \sqrt{c/x}$ singularity at the leading edge. Hence, according to Eq. (29), $h''(x)$ and $v_b'(x)$ both have to contain the same singular factor $\sqrt{(1-X)/X}$ as u. The following expansion for $v_b(X)$ satisfies all of these requirements:

$$\frac{1}{U} v_b'(X) = h''(X) = a\left(\frac{1}{2} - 2X\right)\sqrt{\frac{1-X}{X}} + \sum_{k=1}^{n} kb_k X^{k-1} \tag{30}$$

$$\frac{1}{U} v_b(X) = h'(X) - \alpha = aX^{1/2}(1-X)^{3/2} + \sum_{k=0}^{n} b_k X^k \tag{31}$$

where, to satisfy the Kutta condition at the trailing edge ($X = 1$) in Eq. (29),

$$\sum_{k=1}^{n} kb_k = 0 \tag{32}$$

The lead term of Eq. (30) contains $[(1/2) - 2X]$ and, although not essential, leads to a more compact expression for $v_b(x)$.

The antisymmetrical chordwise velocity component u on the flexible membrane corresponding to the above expansion of $v_b(X)$ is obtained from (17) in the form

$$\frac{1}{4}\Delta C_p = \frac{1}{U} u(X) = -\left\{\frac{a}{\pi}\left[\frac{1}{2} - X + X(1-X)\ln\frac{1-X}{X}\right] + \sum_{k=0}^{n} b_k \sum_{j=0}^{k} g_{k-j} X^j\right\}\sqrt{\frac{1-X}{X}} \tag{33}$$

where g_{k-j} is defined by Eq. (20).

The camber shape of the flexible membrane can be obtained by integrating Eq. (31), in the form

$$h(X) = c\left[\alpha X + aJ_0 + \sum_{k=0}^{n} \frac{b_k}{k+1} X^{k+1}\right] \tag{34}$$

where

$$J_0 = \frac{1}{8}\cos^{-1}\sqrt{1-X} - \sqrt{(1-X)X}\left(\frac{1}{8} - \frac{7}{12}X + \frac{1}{3}X^2\right) \tag{35}$$

There are $(n+2)$ coefficients defining the membrane camber, a and b_k ($k = 0,1,2,\ldots,n$), which have to be determined using the condition (32) and the membrane equilibrium equation (29). At the leading edge ($X = 0$), Eq. (29), which involves u and v_b', reduces to

$$a\frac{1}{2}\left(\frac{1}{\pi} - \frac{1}{4}C_T\right) + \sum_{k=0}^{n} b_k g_k = 0 \tag{36}$$

Other $(n-1)$ equations can be obtained satisfying Eq. (29) at other convenient locations X_i ($i = 1,2,\ldots,n-1$) along the chord

$$u(X_i) = -\frac{1}{4} C_T v'(X_i), \qquad i = 1,2,\ldots,(n-1) \tag{37}$$

The final equation is obtained from (34) by requiring that the chord lies along the x axis, i.e., $h(1) = h(0)$,

$$\frac{\pi}{16} a + \sum_{k=0}^{n} \frac{1}{k+1} b_k = -\alpha \tag{38}$$

Eliminating the coefficient a, using Eq. (38), the system of equations reduces to the form

$$[D_{ik}]\left[\frac{b_k}{\alpha}\right] = [e_i] \tag{39}$$

This can be solved for the coefficients (b_k/α), which are independent of α, provided that the matrix $[D_{ik}]$ is not singular, as, for example, when $C_T = 1.727$, which corresponds to the case

Table 1 Comparison between the present solution for flexible-membrane airfoils and the previous results of Nielsen[9] and Thwaites[10]

C_T		$\alpha/\sqrt{\epsilon}$	α/C_L
	Present method	0.322	28.250
2	Nielsen	0.322	28.148
	Thwaites	0.340	24.989
	Present method	2.434	8.952
4	Nielsen	2.411	8.821
	Thwaites	2.480	8.848
	Present method	6.424	7.255
8	Nielsen	6.329	7.120
	Thwaites	6.400	7.277
	Present method	8.400	7.021
10	Nielsen	8.266	6.884
	Thwaites	8.371	7.120
	Present method	13.33	6.744
15	Nielsen	13.10	6.605
	Thwaites	13.29	6.762
	Present method	96.88	6.345
100	Nielsen	—	—
	Thwaites	96.86	6.349
	Present method	391.69	6.298
400	Nielsen	—	—
	Thwaites	391.83	6.299

of a flexible membrane at an *ideal* incidence, $\alpha=0$. At this *ideal* incidence, $a=0$ and, hence, the pressure distribution, as well as the membrane curvature, do not contain the leading-edge singularity $x^{-1/2}$.

The excess length, defined as $\epsilon=\ell/c-1$, is given by the relation

$$\epsilon=\int_0^1\sqrt{1+\left[\frac{1}{U_\infty}v_b(X)+\alpha\right]^2}\,dX-1$$
$$\simeq\frac{\alpha^2}{2}\int_0^1\left[1+\frac{v_b(X)}{\alpha U}\right]^2 dX \tag{40}$$

and the lift coefficient of the flexible membrane airfoil is expressed, using Eq. (29), as

$$\frac{C_L}{\alpha}=-C_T\sum_{k=1}^{n}\left(\frac{b_k}{\alpha}\right) \tag{41}$$

The results obtained with the present method are compared in Table 1 with the previous results of Nielsen[9] and Thwaites.[10]

These results for the overall parameters α/C_L, $\alpha/\sqrt{\epsilon}$, and C_T are generally in fair agreement, although there are detailed differences. The present method is in good agreement for $C_T>8$ with Thwaites method, which was developed for very high C_T but is less accurate for smaller C_T. The comparison with Nielsen's method shows good agreement for $C_T<8$.

At higher C_T (or higher $\alpha/\sqrt{\epsilon}$), Nielsen's method is expected to become less accurate because his Fourier expansion (27) of the membrane slope fails to provide, when differentiated, the leading-edge singularity $x^{-1/2}$ in the membrane curvature expression. This singularity is important for satisfying the membrane equilibrium equation (24) near the leading edge, which, as mentioned following Eq. (28), Nielsen's method cannot satisfy accurately. However, this singularity is likely to become less important for very small incidences (small $\alpha/\sqrt{\epsilon}$), as C_T approaches the first critical eigenvalue $C_{T_c}=1.727$ (for which there is no leading-edge singularity), in which case Nielsen's results become more accurate and agree well with the present solution. These detailed differences in the behavior of the theoretical solutions are, however, less important practically, due to viscous effects and to separation at the trailing edge and separation bubbles at the leading edge. As a result the potential flow theories compare rather poorly with experiment, as shown by Newman,[17] although agreement improves somewhat as the membrane camber is reduced.

Jet-Flapped Airfoils

Consider a thin cambered airfoil of chord length c, provided with a thin jet flap inclined at an angle β, with respect to the chord, at the trailing edge (Fig. 3b).

The jet is assumed to be a thin sheet and have a small slope,[12-14,19] and to have a constant momentum J per unit length of slot. The sheet curvature $1/R\approx e''(x)$, where $y_J=e(x)$ is the jet-flap shape, is related to the pressure difference across the jet sheet by the momentum equation normal to the jet (note that e is positive in the direction of positive y):

$$\Delta p=J/R\simeq Je''(x) \tag{42}$$

Using the dimensionless jet momentum coefficient $C_J=2J/(\rho U^2c)$, this equation can also be expressed in terms of u and v in a form similar to Eq. (29):

$$(4/C_J)\,u(x)=cv'(x) \tag{43}$$

In addition, the aerodynamic boundary condition (25) has to be satisfied on the airfoil, where $h(x)$ is specified, and furthermore, the same condition has to be satisfied on the jet sheet itself:

$$v=v_J(x)=\left[-\alpha+e'(x)\right]U \tag{44}$$

where the jet flap shape, $y_J=e(x)$, has to be determined.

At the trailing edge ($x=c$), the jet slope with respect to the chord is specified as β, which leads to the additional condition

$$e'(c)=-\tan\beta\simeq-\beta$$

or

$$v(c)=-U\sin(\alpha+\beta)/\cos\beta\simeq-(\alpha+\beta)U \tag{45}$$

Due to the pressure difference across it, the jet sheet is deflected upwards and, eventually, at large distance ℓ behind the airfoil, becomes flat and parallel to the freestream direction. This can be expressed by the additional condition

$$e'(\ell)=e''(\ell)=0$$

or

$$v(\ell)=v'(\ell)=0,\qquad[\text{also } u(\ell)=0] \tag{46}$$

where ℓ tends, theoretically, to infinity. However, the jet curvature practically tends to zero at a finite distance $(\ell-c)$, measured from the trailing edge, which depends on the jet coefficient C_J, the jet angle β, and the incidence α, and, in general, has the same order of magnitude as the chord length c.

In this situation, the jet-flapped airfoil can be considered as a fictitious rigid airfoil of an overall chord length ℓ, with the Kutta condition $u(\ell)=0$ satisfied at $x=\ell$ (where the jet sheet curvature practically tends to zero).

Considering the nondimensional coordinates $X=x/c$ and $L=\ell/c$, the following expansion of the normal-to-chord velocity component on the jet sheet, $v_J(X)$, satisfies the preceding considerations:

$$\frac{1}{U}v_J'(X)=e''(X)=-\sum_{k=2}^{n}e_k\frac{k+1}{X^{k+2}}$$
$$+a\frac{2}{\pi}\sinh^{-1}\sqrt{\frac{L-X}{L(X-1)}} \tag{47}$$

and, by integration,

$$\frac{1}{U}v_J(X)+\alpha=e'(X)=\sum_{k=2}^{n}e_k\frac{1}{X^{k+1}}+aF(X) \tag{48}$$

where $L=\ell/c$, and

$$F(X)=(X-1)\frac{2}{\pi}\sinh^{-1}\sqrt{\frac{L-X}{L(X-1)}}$$
$$-\sqrt{L-1}\,\frac{2}{\pi}\cos^{-1}\sqrt{\frac{X}{L}} \tag{49}$$

The last term of Eq. (47) accounts for the trailing-edge singularity appearing in u when the jet is not tangent to the camberline, i.e., when $h'(1)\neq-\tan\beta\simeq-\beta$ [see Eq. (54)], since v' and u are related by Eq. (43).

The boundary condition regarding the jet slope β at the trailing edge can be expressed in the form

$$\sum_{k=2}^{n}e_k=-\tan\beta-aF(1) \tag{50}$$

and at the other end of the jet sheet ($X=L$), the boundary conditions can be expressed as

$$e'(L)=\sum_{k=2}^{n}e_k/L^{k+1}=0 \tag{51}$$

$$e''(L)=-\sum_{k=2}^{n}(k+1)e_k/L^{k+2}=0 \tag{52}$$

However, since L is usually chosen to be larger than 2, the jet slope at $X=L$ is at least an order of magnitude smaller than the slope at the trailing edge β, and, hence, the conditions (51) and (52) may be omitted in order to avoid having too many terms in the expansion (48).

The antisymmetrical chordwise perturbation velocity component u on the jet-flapped airfoil ($u/U=\Delta C_p/4$) can be obtained using Eq. (17), where the nondimensional coordinates X and S are replaced here by X/L and S/L, and, accordingly, the upper limit of integration will become L, instead of 1; also, $v_b(S)$ in Eq. (17) should correspond to two different variations of the camberline slope on the airfoil itself, $v_b(S)$, and on the jet sheet, $v_J(S)$, i.e.,

$$\frac{1}{U}v_b(S)+\alpha=\begin{cases}\displaystyle\sum_{k=0}^{n}h_kS^k, & \text{for } 0<S<1\\ \displaystyle\sum_{k=2}^{n}e_k\frac{1}{S^{k+1}}+aF(S), & \text{for } 1<S<L\end{cases} \tag{53}$$

where S represents the new nondimensional coordinates with respect to c ($S=s/c$). For convenience, in performing the integration in Eq. (17) on the jet sheet, a polynomial expansion

$$F(S)=\sum_{k=2}^{n}b_k/S^{k+1}$$

is considered, instead of the expression given in Eq. (49).

The value of the chordwise perturbation velocity u on the airfoil and the jet is, thus, obtained as

$$\frac{1}{U}u(X)=\left\{\alpha-\sum_{k=0}^{n}h_k\sum_{j=0}^{k}I_jX^{k-j}-\sum_{k=2}^{n}(e_k+ab_k)\sum_{j=1}^{k}\frac{J_j}{X^{k+1-j}}\right\}\sqrt{\frac{L-X}{X}}$$
$$+\left\{\sum_{k=0}^{n}h_kX^k-\sum_{k=2}^{n}\frac{e_k+ab_k}{X^{k+1}}\right\}\frac{2}{\pi}G(L,1,X) \tag{54}$$

where $G(L,1,X)$ has the expression (14), and I_j and J_j are defined by

$$I_j=-\frac{1}{j}\frac{1}{\pi}\sqrt{L-1}+\frac{2j-1}{2j}LI_{j-1},\quad I_0=1-\frac{2}{\pi}\cos^{-1}\sqrt{\frac{1}{L}} \tag{55}$$

$$J_{j+1}=\frac{2j}{2j+1}\frac{1}{L}\left[\frac{1}{j}\frac{1}{\pi}\sqrt{L-1}+J_j\right],\quad J_1=\frac{1}{L}\frac{2}{\pi}\sqrt{L-1} \tag{56}$$

The constant a, which multiplies the singular term $G(L,1,X)$ at $X=1$, can be determined by applying the jet-momentum equation (43) at the airfoil trailing edge and by considering only the singular terms in $u(X)$ and $v'(X)$. It follows that

$$a=\frac{4}{C_J}\left[\tan\beta+h'(1)\right]\simeq\frac{4}{C_J}\left[\beta+h'(1)\right] \tag{57}$$

When the jet is tangent to the airfoil camberline at the trailing edge, i.e., $\tan\beta=-h'(1)$, then $a=0$ and, hence, the singular behavior of $u(X)$, as well as of $v'(X)$, at $X=1$ ($x=c$) naturally disappears.

The $(n-1)$ unknown coefficients e_k ($k=2,3,\ldots,n$), defining the geometrical shape of the jet sheet, can be determined now by satisfying Eq. (43) at $(n-1)$ convenient locations X_i, situated between $X=1$ and $X=L$, i.e.,

$$u(X_i)=\tfrac{1}{4}C_Jv'(X_i),\qquad (1,2,\ldots,n-1) \tag{58}$$

The boundary condition (50) has also to be added to the system of equations (58) for the determination of the coefficients e_k [as mentioned in the foregoing, conditions (51) and (52) may be omitted].

The present theoretical solution is compared with the solution obtained by Spence[14] and with the experimental results obtained by Dimmock[14] in Fig. 4, which shows the chordwise variation of the nondimensional pressure difference across the airfoil, $\Delta C_p=C_{p_l}-C_{pu}=4u/U$. The present theoretical solution was found to be in good agreement with the experimental results and with Spence's solution.

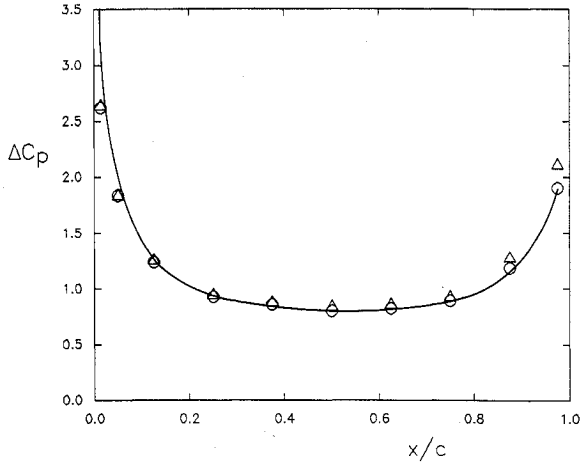

Fig. 4 The present solution (——) for a typical chordwise variation of the nondimensional pressure difference ΔC_p across a jet-flapped airfoil ($\alpha=0$, $\beta=31.4$ deg, $C_j=0.3$) compared with Spence's solution[14] (Δ) and with Dimmock's experimental results[14] (○).

The lift coefficient is obtained by integrating the pressure difference, using Eq. (54), in the form

$$C_L = 4\alpha L \cos^{-1}\sqrt{\frac{L-1}{L}} - 4\left\{\sum_{k=0}^{n} h_k\left[2I_{k+1}\cos^{-1}\sqrt{\frac{L-1}{L}} + \frac{1}{k+1}\sqrt{L-1}\sum_{j=0}^{k} I_j\right] + \sum_{k=2}^{n}(e_k + ab_k)\left[2J_k\cos^{-1}\sqrt{\frac{L-1}{L}} + \frac{1}{k}\sqrt{L-1}\sum_{j=0}^{k-1} J_{j+1}\right]\right\} \tag{59}$$

where I_k and J_k are defined by the Eqs. (55) and (56).

If the airfoil is a flat plate and there is no jet ($h_k = 0$, $C_J = 0$, $\beta = 0$, and in the limit $\beta/C_J = 0$, and, hence, $L = 1$), then only the first term remains in Eq. (59), which reduces to the classical solution $C_L = 2\pi\alpha$. For a flat plate with jet flap, it is not easy to reduce Eq. (59) analytically to the simplified convenient correlations of numerical results proposed by Spence.[11]

The theoretical lift coefficient calculated with the above equation is found to be in good agreement with Dimmock's experimental results and Spence's approximate solution.[11]

Conclusions

A method based on velocity singularities is presented for incompressible potential flow past a thin airfoil. It makes use of special singularities at the airfoil leading edge and ridges (points where the airfoil slope changes), which directly represent the complex perturbation velocity on the airfoil. The method has been developed first for rigid cambered airfoils, starting with a prototype problem represented by a simple flapped airfoil, for which a closed-form solution has been derived.

The method has then been extended to obtain the solution for the flow past flexible impervious membranes and past airfoils with jet flaps. These two problems, apparently different, have in common the fact that the airfoil geometry is not known a priori, since they both depend on the pressure difference across the two sides of the flexible membrane, or the jet sheet. In these cases, special singularities appear in the expression for the normal-to-chord component of the perturbation velocity.

The method of velocity singularities presented in this paper is particularly suitable for solving these special problems, since it can handle directly these normal-to-chord velocity distributions.

The theoretical solutions obtained with the method of velocity singularities are validated first by comparison with the conformal transformation solution for a rigid circular arc airfoil. In addition, the present predictions are compared with those obtained by Nielsen[9] and Thwaites[10,11] for flexible-membrane airfoils and are compared with Spence's solution and the experimental results obtained by Dimmock[11] for jet-flapped airfoils. Agreement is generally very good, and where there are minor differences the present solutions seem to be better, particularly in the case of membrane airfoils.

Acknowledgments

The authors gratefully acknowledge the support of the Natural Sciences and Engineering Council of Canada.

References

[1]Milne-Thomson, L. M., *Theoretical Aerodynamics,* 4th ed., Dover, New York, 1966, pp. 136–145.

[2]Stewart, H. J., "A Simplified Two-Dimensional Theory of Thin Airfoils," *Journal of Aeronautical Sciences,* Vol. 9, No. 12, 1942, pp. 452–456.

[3]Halsey, N. D., "Potential Flow Analysis of Multielement Airfoils using Conformal Mapping," *AIAA Journal,* Vol. 17, No. 12, 1979, pp. 1281–1288.

[4]Hunt, B., "The Panel Method for Subsonic Aerodynamics Flows: A Survey of Mathematical Formulations and Numerical Models and an Outline of the New British Aerospace Scheme," *Von Kármán Institute Lecture Series,* Vol. 1978-4, von Kármán Institute, Brussels, Belgium, March 13–17, 1978.

[5]Mateescu, D., "A Hybrid Panel Method for Aerofoil Aerodynamics," *Boundary Elements XII, Vol. 2, Applications in Fluid Mechanics and Field Problems,* edited by M. Tanaka, C. A. Brebia, and T. Honma, Computational Mechanics Publications, Southampton, England, UK, and Springer-Verlag, Berlin, 1990, pp. 3–14.

[6]Carafoli, E., Mateescu, D., and Nastase, A., "Wing Theory in Supersonic Flow," Pergamon, London, 1969.

[7]Mateescu, D., "Wing and Conical Body of Arbitrary Cross-Section in Supersonic Flow," *Journal of Aircraft,* Vol. 24, No. 4, 1987, pp. 239–247.

[8]Mateescu, D., and Newman, B. G., "Analysis of Flexible-Membrane Aerofoils by a Method of Velocity Singularities," *Proceedings of the Tenth Canadian Congress of Applied Mechanics,* Vol. B, Univ. of Western Ontario, London, Ontario, Canada, 1985, pp. 187, 188.

[9]Nielsen, J. N., "Theory of Flexible Aerodynamic Surfaces," *Journal of Applied Mechanics,* Vol. 30, No. 9, 1963, pp. 435–442.

[10]Thwaites, B., "The Aerodynamic Theory of Sails: Two-Dimensional Sails," *Proceedings of the Royal Society,* Series A, Vol. 261, 1961, pp. 402–422.

[11]Thwaites, B., *Incompressible Aerodynamics,* Oxford Univ. Press, Oxford, England, UK, 1960, pp. 498–505.

[12]Spence, D. A., "The Lift Coefficient of a Thin Jet-Flapped Wing," *Proceedings of the Royal Society,* Series A, Vol. 238, 1956, pp. 46–68.

[13]Spence, D. A., "The Lift of a Thin Aerofoil with a Jet-Augmented Flap," *Aeronautical Quarterly,* Vol. 9, Aug. 1958, pp. 287–299.

[14]Spence, D. A., "Some Simple Results for Two-Dimensional Jet-Flap Aerofoils," *Aeronautical Quarterly,* Vol. 9, Nov. 1958, pp. 395–406.

[15]Kuethe, A. M., and Chow, C.-Y., *Foundations of Aerodynamics,* 4th ed., Wiley, New York, 1986, pp. 122–124.

[16]Newman, B. G., "The Aerodynamics of Flexible Membranes," *Proceedings of the Indian Academy of Sciences,* Vol. 5, 1982, pp. 107–129.

[17]Newman, B. G., "Aerodynamic Theory for Membranes and Sails," *Progressive Aerospace Science,* Vol. 24, 1987, pp. 1–27.

[18]Greenhalgh, S., Curtiss, H. C., and Smith, B., "Aerodynamic Properties of a Two Dimensional Inextensible Flexible Airfoil," *AIAA Journal,* Vol. 22, No. 7, 1984, pp. 865–870.

[19]O'Mahoney, R., and Smith, F. T., "On the Calculation of the Incompressible Flow Past an Aerofoil with a Jet Flap," *Aeronautical Quarterly,* Vol. 29, 1978, pp. 44–59.